SCIENTIFIC REPORTS

OPEN

Crystal-Size Effects on Carbon Dioxide Capture of a Covalently Alkylamine-Tethered Metal-Organic Framework Constructed by a One-Step Self-Assembly

Received: 13 October 2015
Accepted: 11 December 2015
Published: 13 January 2016

Yun Kyeong Kim[1,*], Sung-min Hyun[1,*], Jae Hwa Lee[1], Tae Kyung Kim[1], Dohyun Moon[2] & Hoi Ri Moon[1]

To enhance the carbon dioxide (CO_2) uptake of metal-organic frameworks (MOFs), amine functionalization of their pore surfaces has been studied extensively. In general, amine-functionalized MOFs have been synthesized via post-synthetic modifications. Herein, we introduce a one-step construction of a MOF ([($NiL_{ethylamine}$)(BPDC)] = MOF_{NH2}; $[NiL_{ethylamine}]^{2+} = [Ni(C_{12}H_{32}N_8)]^{2+}$; $BPDC^{2-}$ = 4,4'-biphenyldicarboxylate) possessing covalently tethered alkylamine groups without post-synthetic modification. Two-amine groups per metal centre were introduced by this method. MOF_{NH2} showed enhanced CO_2 uptake at elevated temperatures, attributed to active chemical interactions between the amine groups and the CO_2 molecules. Due to the narrow channels of MOF_{NH2}, the accessibility to the channel of CO_2 is the limiting factor in its sorption behaviour. In this context, only crystal size reduction of MOF_{NH2} led to much faster and greater CO_2 uptake at low pressures.

Global warming by the accumulation of carbon dioxide (CO_2) is a serious environmental problem, because it leads to severe natural disasters[1]. Therefore, the need for practical CO_2 adsorbents is critical, and various efforts have been made in this field[2–4]. Currently, alkylamine solutions are used as CO_2 adsorbents in industry due to their ease of use and low cost[5]. However, ease of degradation, toxic by-products, and a high regeneration energy are endemic problems of this technology[6]. Thus, tethering alkylamine groups on solid supports is considered as a useful strategy to stabilize the amine groups and reduce the energy required for regeneration[4,7–12]. Metal-organic frameworks (MOFs) provide appropriate solid supports due to the chemical tunability of their metal building blocks and organic ligands. To prepare amine-functionalized MOFs, open-metal sites (OMSs) on the internal pore surfaces are decorated with multi-amine molecules to capture CO_2 molecules[13–15]. Physical impregnation of polyalkylamines like polyethyleneimine (PEI) into pore-activated MOFs is also the good approach to introduce active amine groups into the pore[16]. These synthetic methods allow the MOFs to show advanced CO_2 uptake behaviour. However, several preparation steps and leaching of the impregnated amines during multiple regeneration cycles can be potential problems in their practical utilization. Thus, covalent grafting of amine groups on the organic building blocks is very efficient in achieving stable amine-functionalized solid adsorbents[17–19]. However, amino groups substituted to aromatic ligands do not interact strongly with CO_2 due to the electron withdrawing effect of benzene rings[16,20]. Thus, herein we suggest a one-step self-assembly toward a MOF with a pore surface decorated with covalently tethered alkylamines, which can be stable during regeneration. To achieve this synthetic approach, we selected a Ni(II)-complexed macrocycle as a metal building block, which contains two pendant ethylamine groups ($[NiL_{ethylamine}]^{2+} = [Ni(C_{12}H_{32}N_8)]^{2+}$)[21] (Fig. 1a). The amine-tethered MOF shows chemical interactions with CO_2 leading to the formation of ammonium carbamate, which is elucidated by infrared (IR) spectroscopy. In addition, only reducing the crystal size leads at most sevenfold enhancement of CO_2

[1]Department of Chemistry, Ulsan National Institute of Science and Technology (UNIST), 50 UNIST-gil, Ulsan 44919, Republic of Korea. [2]Beamline Division, Pohang Accelerator Laboratory, 80 Jigokro-127-beongil, Nam-gu, Pohang, Gyungbuk 37673, Republic of Korea. *These authors contributed equally to this work. Correspondence and requests for materials should be addressed to H.M. (email: hoirimoon@unist.ac.kr)

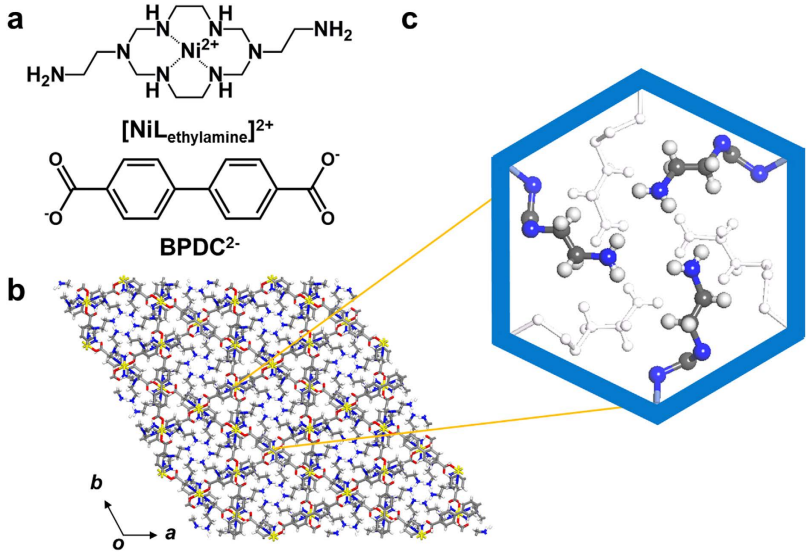

Figure 1. (**a**) Synthetic strategy, and (**b,c**) the structure (ab plane) of a covalently alkylamine-tethered MOF (**MOF$_{NH2}$-as**). (Colour scheme: Ni, yellow; C, grey; O, red; N, blue).

adsorption by increasing the gas accessibility, which resolves the diffusion resistance caused by the high amine density in the pore. Adsorption-desorption cyclic performance is also tested to show the durability of the MOF.

Results and Discussion

X-ray Structure of MOF$_{NH2}$-as. Self-assembly of [NiL$_{ethylamine}$]$^{2+}$ and an organic ligand, BPDC^{2-} yields rod-shaped purple crystals of {[(NiL$_{ethylamine}$)(BPDC)]·3H$_2$O} (**MOF$_{NH2}$-as**). Each Ni^{II} macrocycle has a square planar geometry and acts as a linear linker; its axial sites are coordinated by carboxylate anions from two different BPDC^{2-} ligands in a monodentate fashion, resulting in octahedral centres (Fig. S1). Infinite coordination between BPDC^{2-} and Ni^{II} macrocycles results in one dimensional (1D) chains, which are extended in three different directions. This was similar to a previously reported structure[22], generating honeycomb-like 1D channels. The pendant ethylamine groups are exposed to the 1D channels, decorating the internal pore surface (Fig. 1b,c). Amine moieties from three pendant arms are adjacent to each other in the pore (the shortest distance between amine groups is 2.70 Å), generating a very narrow pore diameter of 1.59 Å. The void volume calculated by PLATON[23] is 612.8 Å^3 (9.1%).

Stability of MOF$_{NH2}$-as. Thermogravimetric analysis (TGA) of **MOF$_{NH2}$-as** (Fig. S2) revealed weight loss up to a temperature of ~230 °C, which was concurrent to the total weight percent of guest water molecules (8.6 wt%) occupying the void spaces. The X-ray powder diffraction (XRPD) pattern of as-synthesized **MOF$_{NH2}$-as** showed strong reflections in the region 5−30°, which were commensurated with the simulated pattern from single crystal X-ray diffraction data (Fig. 2a,b). After heating up to 250 °C under pure N_2 flow, the MOF retained the same structure, showing high thermal stability (Fig. 2c). Since real flue gas usually contains more than 10% (v/v) water and water molecules are very good ligands for metal centres, the water stabilities of MOFs as well as the amine moieties coordinated to the OMSs cannot be assured under humid condition. In the present study, upon suspending the activated MOF in water for 24 h, its structure and the crystallinity were maintained as evidenced by the XRPD pattern (Fig. 2d). Re-activation of the hydrated MOF also resulted in the intact structure as shown in Fig. 2e. Therefore, **MOF$_{NH2}$-as**, in which the amine moieties were tethered by covalent bonds, is a potentially good sorbent due to its thermal and water stability.

Gas Sorption Properties of MOF$_{NH2}$. After activation of the **MOF$_{NH2}$-as** crystals at 90 °C under vacuum for 7 h (**MOF$_{NH2}$**), **MOF$_{NH2}$** maintained the same structure to **MOF$_{NH2}$-as** as evidenced by the XRPD patterns (Fig. S3). N_2 isotherm of **MOF$_{NH2}$** at 77 K showed a type II shape, indicating that the narrow channels (1.59 Å) are not accessible to N_2 molecules (3.64 Å) (Fig. S4). The CO_2 adsorption isotherms for **MOF$_{NH2}$** at several temperatures are depicted in Fig. 3. At 0 °C and 1 bar, **MOF$_{NH2}$** adsorbed a small amount of CO_2 (0.17 mmol g^{-1}). However, as the temperature increased to 100 °C, the CO_2 uptake increased to 1.32 mmol g^{-1} (Table S3). This behaviour is the opposite of what has been observed for previous amine-grafted MOFs, which show a decrease in CO_2 uptake with increasing temperature[14,15]. In the previous reports, owing to their large pores, chemisorption was followed by physisorption, which might be weakened at the higher temperature. On the other hand, **MOF$_{NH2}$** does not have a large enough pore diameter to access multi-layer adsorption, and thus the uptake by physisorption can be exclusively considered. Therefore, at high temperatures the chemisorption in **MOF$_{NH2}$** is much sufficiently occurred to form C-N bonds between amines and CO_2. The desorption isotherms at 0–75 °C did not trace back to the adsorption curve with large hysteresis even in the low-pressure region, and at 100 °C the adsorbed CO_2 molecules were completely desorbed by evacuation (Figs S5 and S6). These different desorption behaviours upon temperatures were verified by the gravimetric uptake result under 100% CO_2 gas flow (Fig. S7). It was found

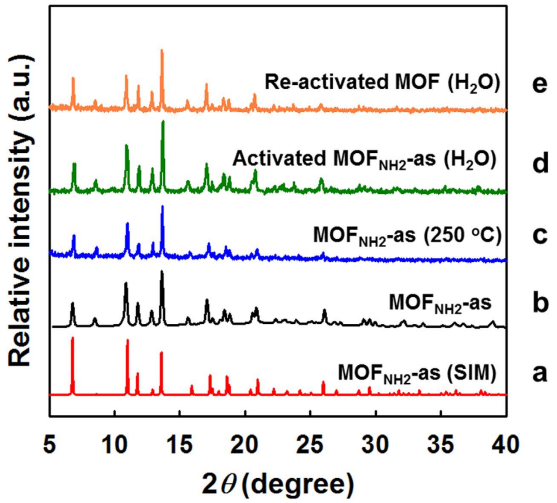

Figure 2. XRPD patterns of (**a**) simulation from single-crystal XRD data of MOF_{NH2}-as, (**b**) MOF_{NH2}-as, (**c**) MOF_{NH2}-as after heating at 250 °C and (**d**) the activated MOF after immersing in water for 24 h (hydrated MOF). (**e**) Re-activated MOF of the hydrated MOF.

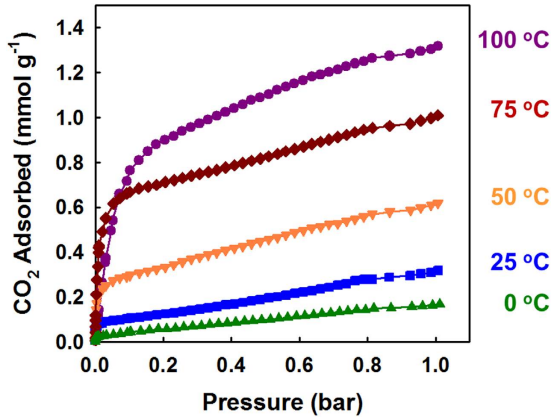

Figure 3. CO_2 adsorption isotherms of MOF_{NH2} obtained at the various temperatures.

that adsorption and desorption are at the equilibrium around 100 °C, and thus the chemisorbed CO_2 molecules in $\mathbf{MOF_{NH2}}$, can be liberated at 100 °C upon pressure reduction.

As described previously, the pore size of $\mathbf{MOF_{NH2}}$ is only half of the kinetic diameter of CO_2 (3.3 Å). Then, how the CO_2 adsorption can occur in this MOF? The flexible movement of the pendant alkylamine groups may allow the uptake of CO_2. At the low temperature, 100 K, at which X-ray single crystal data was collected, the alkylamine groups did not show significant thermal disorderness. However, as the temperature increases, thermal motion of the alkylamines, which have conformational flexibility, become active. Consequently, at certain moments the thermal disorderness makes the pores accessible to CO_2 molecules. Therefore, higher temperatures afford not only stochastically more possibilities to generate a suitable pore size, but also thermal energy to produce chemical bonds between the amino groups and CO_2.

Crystal Size Effects on CO_2 Uptake of MOF_{NH2}. Based on this understanding, the access of CO_2 into the MOF is of critical importance. Accordingly, we compared the CO_2 sorption behaviours of $\mathbf{MOF_{NH2}}$ with the different crystal size, $\mathbf{MOF_{NH2:crystal}}$, which have been treated so far, and well-ground $\mathbf{MOF_{NH2}}$ powder ($\mathbf{MOF_{NH2:powder}}$). $\mathbf{MOF_{NH2:powder}}$ was prepared by pulverizing $\mathbf{MOF_{NH2:crystal}}$, using a sample grinder with stainless steel vial and ball. As shown in the scanning electron microscope (SEM) images (Fig. 4), $\mathbf{MOF_{NH2:crystal}}$ are several tens of micrometres long (average $58.7 \pm 27.8\,\mu m$ measured from 71 crystals), whilst the size of $\mathbf{MOF_{NH2:powder}}$ (average $15.4 \pm 12.0\,\mu m$ measured from 90 crystals) is mainly distributed in a few micrometre range. Interestingly, the only reduction in crystal size of $\mathbf{MOF_{NH2}}$ resulted in much faster and greater CO_2 adsorption (Fig. 5a, S8, and Table S3). The uptake of $\mathbf{MOF_{NH2:powder}}$ at 1 bar were greater by a factor of 1.3–7.5 than those of $\mathbf{MOF_{NH2:crystal}}$ over all temperatures. This might be attributed to a decrease of the channel length in each grain of the adsorbent, which results in high accessibility under the same condition. In contrast with $\mathbf{MOF_{NH2:crystal}}$, $\mathbf{MOF_{NH2:powder}}$ adsorbed the almost same CO_2 uptake at 75 and 100 °C (~7.6 wt%). This suggests that under the guaranteed condition of the CO_2 accessibility, the uptake of ~1.75 mmol g^{-1} might be the maximum value in this MOF. The relatively slow kinetics

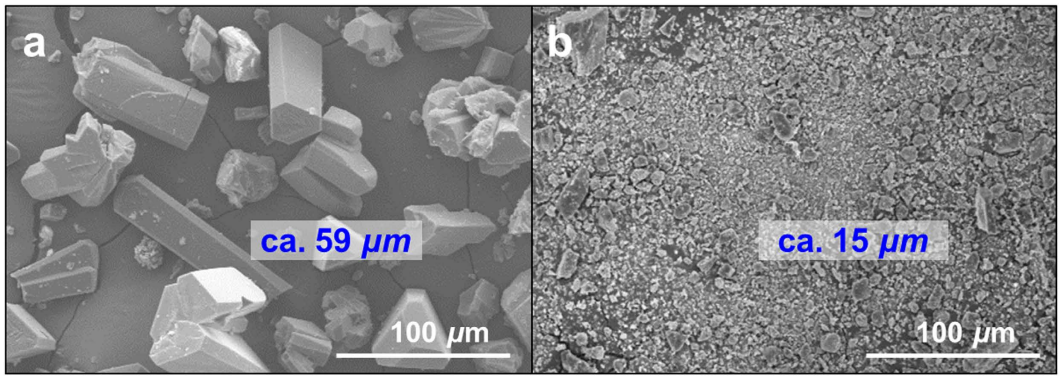

Figure 4. Scanning electron microscope (SEM) images of (**a**) as-synthesized MOF_{NH2} crystals ($MOF_{NH2:crystal}$), and (**b**) MOF_{NH2} after grinding ($MOF_{NH2:powder}$).

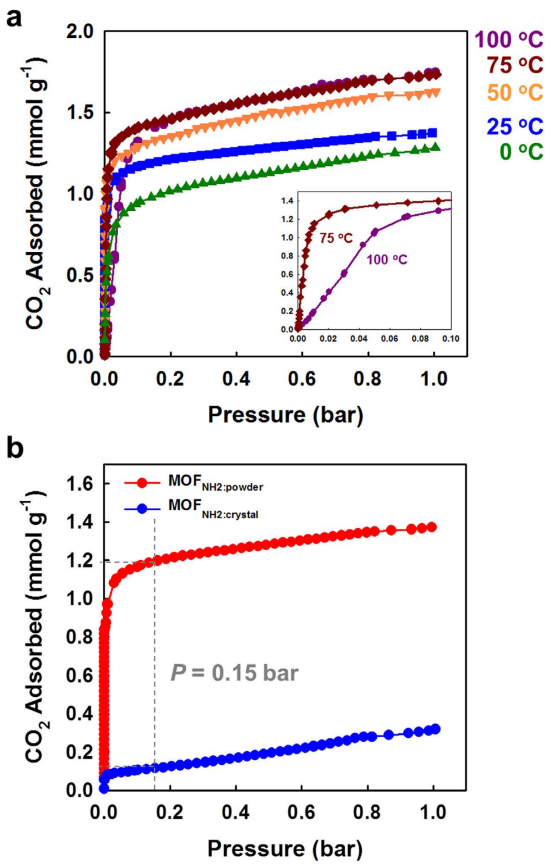

Figure 5. CO_2 adsorption isotherms of (**a**) $MOF_{NH2:powder}$ obtained at the various temperatures. (**b**) Comparison of the CO_2 adsorption behaviour of $MOF_{NH2:crystal}$ and $MOF_{NH2:powder}$ at 25 °C.

was observed at 100 °C because the adsorption and desorption are at the equilibrium around 100 °C as mentioned previously (Fig. 5a inset, and S9). At 0.15 bar and 25 °C, comparable to the CO_2 partial pressure of a typical post-combustion flue gas[24], the CO_2 uptake of $\mathbf{MOF_{NH2:powder}}$ and $\mathbf{MOF_{NH2:crystal}}$ are 1.19 and 0.12 mmol g^{-1}, respectively (Fig. 5b). In other words, the sorption ability at 0.15 bar improved tenfold with a decrease in crystal size. Our result shows the good agreement with that of the amine-modified mesoporous silicas. Sayari group reported the effect of the pore length on CO_2 adsorption in the porous silica with high loading of PEI[25]. SBA-15PLT silica with very short pore channels showed much enhanced adsorption and desorption kinetics as well as low temperature CO_2 uptake. It is obvious that high amine loading is necessarily required for high CO_2 uptake. However, it always comes with diffusion limitation, and thus, the optimization of the loading amount ought to be accompanied. In this context, the reduction of the pore length can be the simple but effective way to enhance the sorption behaviour, and our study is the first report of this trial using MOFs.

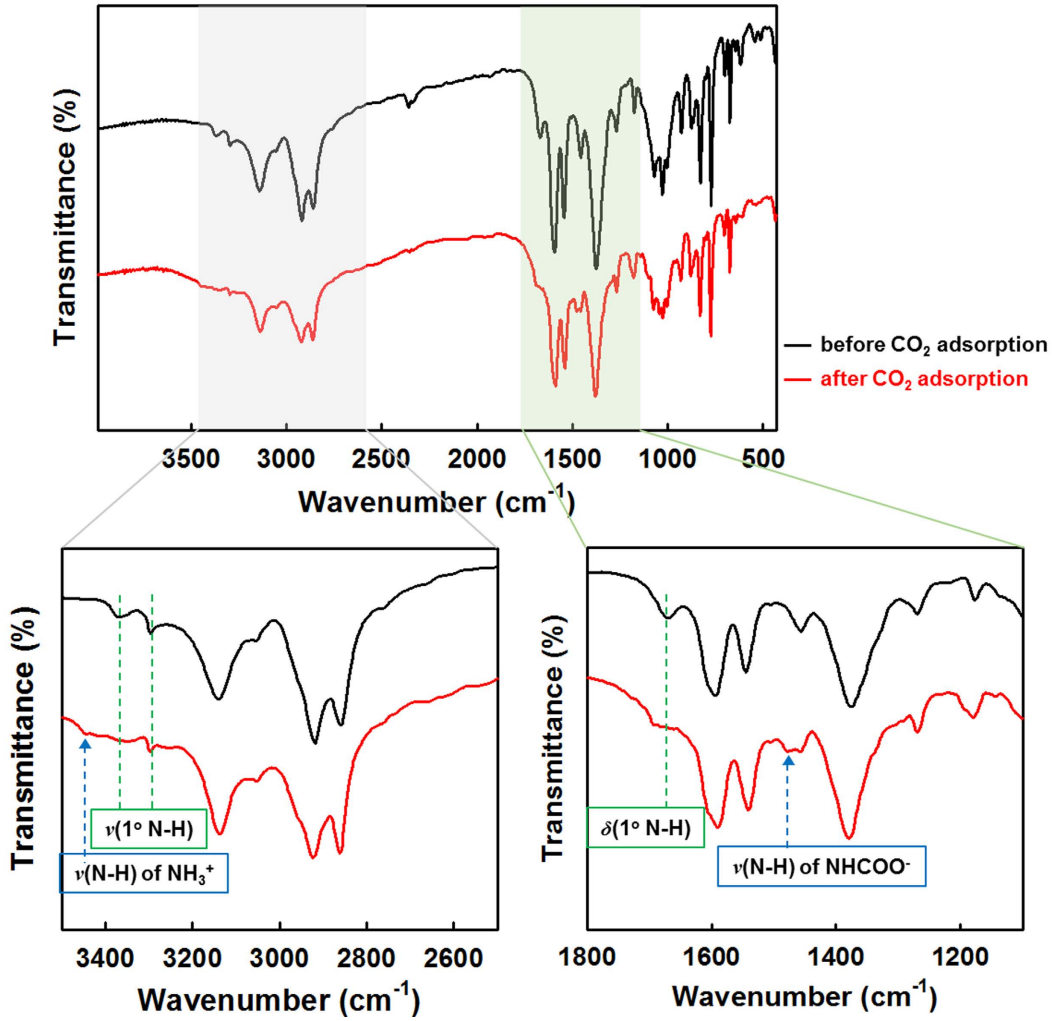

Figure 6. Infrared spectra for $MOF_{NH2:powder}$ before (black) and after (red) adsorbing CO_2.

Evidence of Chemical Interaction between $MOF_{NH2:powder}$ and CO_2. To verify the chemical interaction between CO_2 molecules and the pendant amine groups, the IR spectra of $\mathbf{MOF_{NH2:powder}}$ before and after CO_2 adsorption were compared (Fig. 6). Upon CO_2 adsorption at 75 °C, the stretching bands at 3368, 3293 cm^{-1} and bending band at 1660 cm^{-1}, which correspond to the primary amine (N-H) tethered to the MOF mostly disappeared, remaining the small trace. Simultaneously, new peaks were observed at 3444 cm^{-1} and 1478 cm^{-1}, assigned to N-H stretching of carbamate ($NHCOO^-$) group and NH_3^+ deformation, respectively[26,27]. This result indicated that the chemical interactions between CO_2 and $\mathbf{MOF_{NH2:powder}}$ form ammonium carbamate, which results from a 2:1 amine:CO_2 stoichiometric reaction (equation (1)).

$$2RNH_2 + CO_2 \rightarrow RNH_3^+ + RNHCOO^- \text{(carbamate)} \quad (1)$$

The secondary amine (N-H) peak from the Ni^{II} macrocycle at 3135 cm^{-1} was maintained, showing that CO_2 reacts with only the primary amine of the pendant in the MOF. A 600 MHz ^{13}C NMR analysis also supports the formation of carbamate as a result of the chemical interaction between amine groups and CO_2 molecules (Fig. S10). Unlike the spectra of $\mathbf{MOF_{NH2}}$ before adsorption and after regeneration, that of $\mathbf{MOF_{NH2}}$ adsorbing CO_2 molecules show the distinct peak at 160.5 ppm. Because a carbamic acid C = O resonance is usually observed at 157–160 ppm and carbamate at 164–165 ppm[28,29], the obseved peak might be the result of the equilibrium between carbamate and carbamic acid groups through proton transfer in the solution state. The formed carbamate groups can block the narrow pore to prevent the diffusion of the next CO_2 molecules. However, from the maximum CO_2 uptake amount, the pendants terminated by carbamate or ammonium groups might be expected to have the flexible motions to provide the accessible pathway to CO_2 molecules including the conformational changes of alkyl chains. The isosteric heat of adsorption (Q_{st}) by using CO_2 adsorption data at 50 and 75 °C was calculated by applying a single site Langmuir-Freundlich model (Figs S11 and S12), because the chemisorption is major contribution to the total uptake at those temperatures. Q_{st} is −59.5 kJ mol^{-1} at zero coverage, which is reasonable but relatively small value for the chemisorbed CO_2 in MOF.

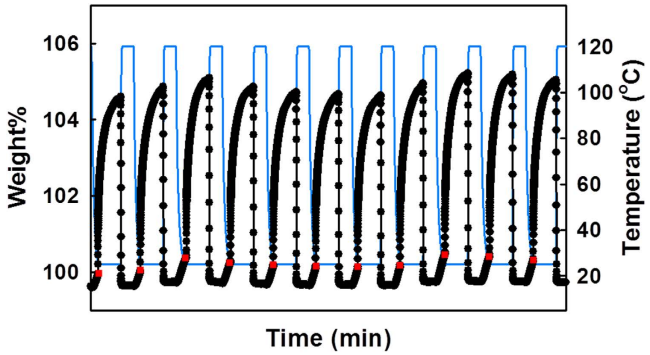

Figure 7. Adsorption-desorption cyclic performance for $MOF_{NH2:powder}$, showing reversible uptake from simulated flue gas (15% CO_2 balanced with N_2). CO_2 was introduced at the red points.

CO_2 Cyclic Performance for $MOF_{NH2:powder}$. Since durability of CO_2 adsorbents is very important for practical applications, adsorption-desorption cyclic performance of **$MOF_{NH2:powder}$** was tested by using TGA with a combined temperature swing and nitrogen purge approach (Fig. 7). The sample was activated at 150 °C under pure N_2 flow for 7 h. Then, a simulated flue gas was introduced into the furnace for 2 h at 25 °C, followed by regeneration at 120 °C for 1 h under pure N_2 gas. A CO_2 uptake capacity of 4.80 wt% (1.09 mmol g^{-1}) was recorded on an average over 12 cycles, and there was no decrease in CO_2 uptake, indicating that the CO_2 adsorption ability of **$MOF_{NH2:powder}$** is maintained over repeated cycling.

Conclusions

In conclusion, an amine-functionalized MOF, **MOF_{NH2}**, was successfully synthesized via a one-step construction method. The structure of **MOF_{NH2}** was determined by using single-crystal XRD, confirming that the covalently tethered alkylamine groups conserved the loading of amine groups as two per metal centre. **MOF_{NH2}** showed enhanced CO_2 adsorption as temperature increases, and the results of sorption experiments and IR spectroscopy revealed that chemisorption occurred through the interaction between CO_2 molecules and amine groups. Since the narrow channel in the MOF restricts the easy access of CO_2 molecules, reducing the crystal size led faster and greater CO_2 adsorption under same sorption condition with diminished diffusion resistance and enhanced amine accessibility inside the pores. The chemical interaction between the primary amine groups tethered to the MOF and CO_2 molecules formed ammonium carbamate, which was reversibly dissociated at mild temperature, 100 °C, to release CO_2 molecules. **MOF_{NH2}** was found to be a renewable CO_2 adsorbent with good stability over repeated cycling.

Methods

Materials and Methods. All chemicals and solvents used in the syntheses were of reagent grade and were used without further purification. $[NiL_{ethylamine}](ClO_4)_2$ was prepared by a reported method with minor modifications[21]. Infrared spectra were measured on a Thermo Fisher Scientific Nicolet 6700 FT-IR spectrometer. Thermogravimetric analyses (TGA) were performed under N_2 at a scan rate of 5 °C/min and under pure CO_2 at a scan rate of 1 °C/min using a Q50 from TA instruments. XRPD data were collected using both a Bruker D2 PHASER automated diffractometer at 30 kV and 10 mA for Cu Kα (λ = 1.54050 Å), with a step size of 0.02° in 2θ and an ADSC Quantum-210 detector at 2D SMC with a silicon (111) double crystal monochromator (DCM) at the Pohang Accelerator Laboratory, Korea. Scanning electron microscope (SEM) images were taken using a Quanta 200 microscope (FEI) operating at 18 kV. The gas sorption data were collected by using a BELsorp-MAX. UV/Vis diffuse reflectance spectra were recorded on a Cary 5000 UV/Vis spectrophotometer. Nuclear magnetic resonance (NMR) spectra were recorded on a Varian VNMRS 600 spectrometer. Elemental analyses were conducted by UNIST Central Research Facilities centre (UCRF) in Ulsan National Institute of Science and Technology (UNIST).

Synthesis of MOF_{NH2}-as, {[($NiL_{ethylamine}$)(BPDC)]·$3H_2O$}. $[NiL_{ethylamine}](ClO_4)_2$ (0.04 g, 0.07 mmol) and Na_2BPDC (0.02 g, 0.07 mmol) were dissolved in *N,N*-diethylformamide (4 mL) and in a mixed solution of acetonitrile (MeCN) and H_2O (MeCN:H_2O = 2 mL:1 mL), respectively. The solution of Na_2BPDC was diffused onto the former solution and powder was formed at the boundary of the layered solution prior to the formation of crystals. The mixed solution allowed to stand at room temperature for 1 day until the pale purple crystals were formed along with some powder. Only crystals were used for analyses. Yield: 22.7%. FT-IR (KBr): 3368 and 3293 cm^{-1} (NH), 3062 cm^{-1} (CH), 1587 cm^{-1} and 1379 cm^{-1} (COO^-); UV-Vis (diffuse reflectance spectrum): λ_{max} 517 nm (Ni^{II} d-d transition); Elemental analysis calcd., found for $Ni_1C_{26}H_{46}N_8O_7$: C (48.69, 49.36), H (7.23, 7.10), N (17.47, 17.52).

Preparation of $MOF_{NH2:crystal}$ and $MOF_{NH2:powder}$. The as-synthesized compounds, **MOF_{NH2}-as**, were heated at 90 °C under vacuum for 7 h, and then cooled to an ambient temperature and refilled with Ar (**$MOF_{NH2:crystal}$**). To prepare the powder samples (**$MOF_{NH2:powder}$**), **MOF_{NH2}-as** was pulverized for 10 s using

a sample grinder with a stainless steel vial and ball (ShakIR sample grinder, PIKE), which is usually used for preparation of infrared spectroscopy samples. The resultant powder was also activated at 90 °C for 7 h, yielding $\mathbf{MOF_{NH2:powder}}$.

Single-Crystal X-ray crystallography. Single-crystals of $\mathbf{MOF_{NH2}}$**-as** were coated with paratone-*N* oil because they lost their crystallinity upon exposure to the air. The diffraction data of $\mathbf{MOF_{NH2}}$**-as** were measured at 100 K using synchrotron employing a PLSII-2D SMC an ADSC Quantum-210 detector with a silicon (111) double crstal monochromator (DCM) at Pohang Accelerator Laboratory, Korea. The ADSC Q210 ADX program[30] was used for both data collection, and HKL3000sm (Ver. 703r)[31] was used for cell refinement, reduction and absorption correction. The structures of $\mathbf{MOF_{NH2}}$**-as** were solved using direct methods with SHELX-XS (Ver. 2008) and refined by full-matricx least-squares calculation with SHELX-XL (Ver. 2008) program package[32]. An half of ligands, an half of Ni ions and one unligated water molecule were observed as an asymmetric unit. For the structure $\mathbf{MOF_{NH2}}$**-as**, the alkyl amine pendant group was restrained using ISOR during the least-squares refinement. All non-hydrogen atoms in whole structures were refined anisotropically and hydrogen atoms were assigned geometrically using a riding model. Refinement of the structure $\mathbf{MOF_{NH2}}$**-as** converged at a final $R_1 = 0.0709$, $wR_2 = 0.2208$ for 18729 reflections with $I > 2\sigma(I)$; $R_1 = 0.0776$, $wR_2 = 0.2294$ for all reflections. The largest difference peak and hole were 0.959 and -0.543 e·Å^{-3}, respectively. A summary of the crystals and some crystallographic data are given in Table S1 and S2. CCDC 1044896 contains the supplementary crystallographic data. The data can be obtained free of charge at www.ccdc.cam.ac.uk/conts/retrieving.html or from the Cambridge Crystallographic Data Centre, 12, Union Road, Cambridge CB2 EX, UK.

References

1. Quadrelli, R. & Peterson, S. The energy–climate challenge: Recent trends in CO_2 emissions from fuel combustion. *Energy policy* **35,** 5938–5952 (2007).
2. Haszeldine, R. S. Carbon capture and storage: how green can black be? *Science* **325,** 1647–1652 (2009).
3. Sumida, K. *et al.* Carbon dioxide capture in metal-organic frameworks. *Chem. Rev.* **112,** 724–781 (2012).
4. Wang, J. *et al.* Recent advances in solid sorbents for CO_2 capture and new development trends. *Energy Environ. Sci.* **7,** 3478–3518 (2014).
5. Rochelle, G. T. Amine scrubbing for CO_2 capture. *Science* **325,** 1652–1654 (2009).
6. Notz, R., Tonnies, I., McCann, N., Scheffknecht, G. & Hasse, H. CO_2 capture for fossil fuel-fired power plants. *Chem. Eng. Technol.* **34,** 163–172 (2011).
7. Goeppert, A. *et al.* Carbon dioxide capture from the air using a polyamine based regenerable solid adsorbent. *J. Am. Chem. Soc.* **133,** 20164–20167 (2011).
8. Chaikittisilp, W., Kim, H. J. & Jones, C. W. Mesoporous alumina-supported amines as potential steam-stable adsorbents for capturing CO_2 from simulated flue gas and ambient air. *Energy Fuels*. **25,** 5528–5537 (2011).
9. Gebald, C., Wurzbacher, J. A., Tingaut, P., Zimmermann, T. & Steinfeld, A. Amine-based nanofibrillated cellulose as adsorbent for CO_2 capture from air. *Environ. Sci. Technol.* **45,** 9101–9108 (2011).
10. Leal, O., Bolivar, C., Ovalles, C., Garcia, J. J. & Espidel, Y. R. Reversible adsorption carbon dioxide on amine surface-bonded silica gel. *Inorg. Chim. Acta.* **240,** 183–189 (1995).
11. Harlick, P. J. E. & Sayari, A. Applications of pore-expanded mesoporous silica. 3. Triamine silane grafting for enhanced CO_2 adsorption. *Ind. Eng. Chem. Res.* **45,** 3248–3255 (2006).
12. Du, Y. *et al.* Carbon dioxide adsorbent based on rich amines loaded nano-silica. *J. Colloid Interface Sci.* **409,** 123–128 (2013).
13. Hu, Y., Verdegaal, W. M., Yu, S. H. & Jiang, H. L. Alkylamine-tethered stable metal–organic framework for CO_2 capture from flue gas. *ChemSusChem* **7,** 734–737 (2014).
14. Lee, W. R. *et al.* Diamine-functionalized metal–organic framework:exceptionally high CO_2 capacities from ambient air and flue gas, ultrafast CO_2 uptake rate, and adsorption mechanism. *Energy Environ. Sci.* **7,** 744–751 (2014).
15. McDonald, T. M. *et al.* Capture of carbon dioxide from air and flue gas in the alkylamine-appended metal−organic framework mmen-Mg_2(dobpdc). *J. Am. Chem. Soc.* **134,** 7056–7065 (2012).
16. Lin, Y., Yan, Q., Kong, C. & Chen, L. Polyethyleneimine incorporated metal-organic frameworks adsorbent for highly selective CO_2 capture. *Sci. Rep*. **3,** 1859–1865 (2013).
17. Ko, N. *et al.* A significant enhancement of water vapour uptake at low pressure by amine-functionalization of UiO-67. *Dalton Trans.* **44,** 2047–2051 (2015).
18. Couck, S. *et al.* An amine-functionalized MIL-53 metal-organic framework with large separation power for CO_2 and CH_4. *J. Am. Chem. Soc.* **131,** 6326–6327 (2009).
19. Lu, W. *et al.* Polyamine-tethered porous polymer networks for carbon dioxide capture from flue gas. *Angew. Chem. Int. Ed.* **51,** 7480–7484 (2012).
20. Brune, S. N. & Bobbitt, D. R. Role of electron-donating/withdrawing character, pH, and stoichiometry on the chemiluminescent reaction of Tris (2,2′-bipyridyl) ruthenium (III) with Amino Acids. *Anal. Chem.* **64,** 166–170 (1992).
21. Kang, S. G., Ryu, K., Jung, S. K. & Kim, J. Template synthesis, crystal structure, and solution behavior of a hexaaza macrocyclic nickel (II) complex containing two N-aminoethyl pendant arms. *Inorganica Chimica Acta.* **293,** 140–146 (1999).
22. Moon, H. R., Kim, J. H. & Suh, M. P. Redox-active porous metal-organic framework producing silver nanoparticles from Ag^I ions at room temperature. *Angew. Chem. Int. Ed.* **44,** 1261–1265 (2005).
23. Sluis, P. V. D. & Spek, A. L. BYPASS: an effective method for the refinement of crystal structures containing disordered solvent regions. *Acta Cryst.* **A46,** 194–201 (1990).
24. Granite, E. J. & Pennline, H. W. Photochemical removal of mercury from flue gas. *Ind. Eng. Chem. Res.* **41,** 5470–5476 (2012).
25. Heydari-Gorji, A., Yang, Y. & Sayari, A. Effect of the pore length on CO_2 adsorption over amine-modified mesoporous silicas. *Energy Fuels* **25,** 4206–4210 (2011).
26. Bacsik, Z. *et al.* Mechanisms and kinetics for sorption of CO_2 on bicontinuous mesoporous silica modified with n-propylamine. *Langmuir* **27,** 11118–11128 (2011).
27. Danon, A. Stair, P. C. & Weitz, E. FTIR Study of CO_2 Adsorption on amine-grafted SBA-15: elucidation of adsorbed species. *J. Phys. Chem. C* **115,** 11540–11549 (2011).
28. Ballard, M., Bown, M., James, S. & Yang, Q. NMR studies of mixed amines. *Energy Procedia* **4,** 291–298 (2011).
29. Kortunov, P. V., Siskin, M., Baugh, L. S. & Calabro, D. C. In situ nuclear magnetic resonance mechanistic studies of carbon dioxide reactions with liquid amines in non-aqueous systems: evidence for the formation of carbamic acids and zwitterionic species. *Energy Fuels* **29,** 5940–5966 (2015).
30. Arvai, A. J. & Nielsen, C. *ADSC Quantum-210 ADX Program*; Area Detector System Corporation: Poway, CA, USA (1983).

31. Z. Otwinowski, W. Minor and C. W. Carter Jr, Sweet (Eds.), R. M. Methods in Enzymology 276 Part A; Academic Press: New York, **307** (1997).
32. Sheldrick, G. M. *SHELXTL-PLUS: Crystal Structure Analysis Package*; Bruker Analytical X-Ray: Madison, WI, USA (1997).

Acknowledgements

We acknowledge financial support from the Korea CCS R&D Centre (KCRC) grant funded by the Korea government (Ministry of Science, ICT & Future Planning) (NRF-2014M1A8A1049255) and Basic Science Research Program through the National Research Foundation of Korea (NRF) funded by the Ministry of Education, Science and Technology (NRF-2013R1A1A3010846).

Author Contributions

Y.K.K., S.-m.H. and H.R.M. designed the experiments. Y.K.K., S.-m.H. and T.K.K. conducted experiments and analyzed data. J.H.L. performed the NMR analysis. D.M. supported the synchrotron experiments. H.R.M. wrote the manuscript. All authors reviewed the manuscript.

Additional Information

Supplementary information accompanies this paper at http://www.nature.com/srep

Competing financial interests: The authors declare no competing financial interests.

How to cite this article: Kim, Y. K. *et al.* Crystal-Size Effects on Carbon Dioxide Capture of a Covalently Alkylamine-Tethered Metal-Organic Framework Constructed by a One-Step Self-Assembly. *Sci. Rep.* **6**, 19337; doi: 10.1038/srep19337 (2016).